

A Luminous Lyman- α Emitting Galaxy at Redshift $z=6.535$: Discovery and Spectroscopic Confirmation¹

James E. Rhoads ^{2,3}, Chun Xu ², Steve Dawson ⁶, Arjun Dey ⁴, Sangeeta Malhotra ^{2,3}, JunXian Wang ⁵, Buell T. Jannuzzi ⁴, Hyron Spinrad ⁶, Daniel Stern ⁷

ABSTRACT

We present a redshift $z = 6.535$ galaxy discovered by its Lyman- α emission in a 9180Å narrowband image from the Large Area Lyman Alpha (LALA) survey. The Lyman- α line luminosity (1.1×10^{43} erg s $^{-1}$) and rest frame equivalent width ($> 100\text{\AA}$) are among the largest known for star forming galaxies at $z \approx 6.5$. Because a neutral intergalactic medium (IGM) suppresses the Lyman- α equivalent width and luminosity, the detection of this galaxy is most easily explained if the IGM is mostly ionized at $z \approx 6.5$. We also present complete spectroscopic followup of the remaining candidates with line flux $> 2 \times 10^{-17}$ erg cm $^{-2}$ s $^{-1}$ in our 1200Å narrowband image. These include another galaxy with a strong emission line at 9136Å and no detected continuum flux, which however is most likely an [O III] $\lambda 5007$ source at $z = 0.824$ based on a weak detection of the [O III] $\lambda 4959$ line.

Subject headings: galaxies: high-redshift — galaxies: formation — galaxies: evolution — cosmology: observations — early universe

²Space Telescope Science Institute, 3700 San Martin Drive, Baltimore, MD 21218; email: rhoads, san, chunxu@stsci.edu

³Visiting Astronomer, Kitt Peak National Observatory.

⁴National Optical Astronomy Observatory, 950 N. Cherry Ave., Tucson, AZ 85719; email: adey, bjannuzzi@noao.edu

⁵Johns Hopkins University, Charles and 34th Street, Bloomberg Center, Baltimore, MD 21218

⁶University of California, Berkeley, CA; email: sdawson, spinrad @astro.berkeley.edu

⁷NASA Jet Propulsion Laboratory, Pasadena, CA, email: stern@zwolfkinder.jpl.nasa.gov

¹The data presented in this paper were obtained at the Kitt Peak National Observatory, the Gemini Observatory, and the W. M. Keck Observatory. Kitt Peak National Observatory, National Optical Astronomy Observatory, is operated by the Association of Universities for Research in Astronomy, Inc. (AURA) under cooperative agreement with the National Science Foundation (NSF). The Gemini Observatory is operated by AURA under a cooperative agreement with the NSF on behalf of the Gemini partnership: the National Science Foundation (United States), the Particle Physics and Astronomy Research Council (United Kingdom), the National Research Council (Canada), CONICYT (Chile), the Australian Research Council (Australia), CNPq (Brazil) and CONICET (Argentina). The W. M. Keck Observatory is operated as a scientific partnership among the California Institute of Technology, the University of California and the National Aeronautics and Space Administration. The Keck Observatory was made possible by the generous financial support of the W.M. Keck Foundation.

1. Introduction

Observational study of the redshift range $6 \lesssim z \lesssim 7$ is crucial for understanding the reionization of intergalactic hydrogen, which was the last major phase transition for most of the baryonic matter in the universe. While polarization of the microwave background measured by the Wilkinson Microwave Anisotropy Probe (WMAP) satellite indicates that substantial ionization had begun as early as $z \sim 15$ (Spergel et al. 2003), both the opaque Gunn-Peterson troughs observed in the spectra of $z \gtrsim 6.3$ quasars (Becker et al. 2001; Fan et al. 2002) and the high temperature of the intergalactic medium at $z \sim 4$ (Theuns et al. 2002; Hui & Haiman 2003) imply that a large part of the reionization was relatively recent, with substantial neutral gas lasting up to $z \sim 6$.

Lyman- α emission has proven the most effective tool so far for identifying star forming galaxies at redshifts $z > 6$; indeed, all but two of the ~ 6 galaxies that have been spectroscopically confirmed at $z > 6$ were found through their Lyman- α line emission in either narrowband or spectroscopic searches (Hu et al 2002; Kodaira et al 2003; Cuby et al 2003; this work; Kneib et al 2004).

In this Letter, we present the extension of the Large Area Lyman Alpha (LALA) survey to the $z \approx 6.5$ window. We have obtained spectra for each of the three $z \approx 6.5$ candidates that pass all photometric selection criteria. Two of these show strong emission lines in the narrowband filter bandpass. In one case, the line is identified as Lyman- α at $z \approx 6.535$ based on its asymmetric profile and the absence of other detected lines down to faint flux levels. The second object is identified as an [O III] $\lambda 5007$ source at $z \approx 0.824$ based on a probable (4σ) detection of the [O III] $\lambda 4959$ line.

2. Imaging Observations and Analysis

The LALA survey's $z \approx 6.5$ search is based on a deep 9180Å narrowband image of our Boötes field, which is $36' \times 36'$ with center at $14:25:57 +35:32$ (J2000.0). The image was obtained using the CCD Mosaic-1 Camera at the 4m Mayall Telescope of the Kitt Peak National Observatory together with a custom narrowband filter, whose central wavelength of $\lambda_c \approx 9182\text{\AA}$ and full width at half maximum (FWHM) of 84\AA place it in a gap between the night sky airglow lines.

Narrowband imaging data were obtained on UT 2001 June 15–17 and 24–25 and 2002 April 5 and 18–19. The total exposure time was 28 hours.

Data reduction followed the same procedures used in the $z = 4.5$ and $z = 5.7$ LALA images (Rhoads et al. 2000; Rhoads & Malhotra 2001). To summarize, we remove electronic crosstalk between Mosaic chip pairs sharing readout electronics; subtract overscan and bias frame corrections; and flatfield with dome flats. Next, we subtract a pupil ghost image caused by internal reflections in the KPNO 4m corrector. We remove residual, large scale imperfections in the sky flatness using a smoothed supersky flat derived from the science data, followed by subtraction of a polynomial surface fit to the sky flux. A fringe frame was constructed from the data, fitted to the blank sky regions of each exposure, and subtracted. Cosmic rays were rejected in each exposure using the

algorithm of Rhoads (2000).

The world coordinate systems of individual frames were adjusted to the USNO-A2 star catalog (Monet et al 1998). Satellite trails were flagged by hand for exclusion from the final stacks. The eight-chip Mosaic-1 images were then mapped onto a rectified, common coordinate grid using the “mscimage” task from the IRAF MSCRED package (Valdes & Tody 1998; Valdes 1998). The seeing, throughput, and sky brightness in each exposure were measured and used to compute a set of weights for image stacking using the “ATTWEIGHT” algorithm (Fischer & Kochanski 1994). Finally, the exposures were stacked, with an additional sigma clipping applied to reject discrepant data not previously flagged. The majority of the weight comes from the final two nights’ imaging data, and only 24% of the total weight is from the 2001 observing season.

The final stack has seeing $1.02''$ and a 5σ sensitivity limit of $0.7\mu\text{Jy}$ (measured within a 9 pixel [$2.32''$] diameter aperture), corresponding to $2.0 \times 10^{-17} \text{ erg cm}^{-2} \text{ s}^{-1}$ for a pure line source at these wavelengths or to an AB magnitude of 24.3 for a pure continuum source. The magnitude zero point was determined by comparison with a deep z' filter image obtained earlier (see Rhoads & Malhotra 2001), which was in turn calibrated to z' filter standard stars from SDSS standard star lists.

3. Candidate Selection

Lyman- α galaxy candidates were selected following the criteria used successfully in lower redshift LALA searches (Rhoads & Malhotra 2001; Dawson et al. 2004). In summary, these include: 1) Significance of the narrowband detection $> 5\sigma$; 2) A narrowband excess of at least 0.75 magnitude, so that $\geq 50\%$ of the narrowband flux comes from an emission line; 3) Significance of the narrowband excess $> 4\sigma$; and 4) No detection in filters blueward of the expected Lyman break location at the $< 2\sigma$ level.

To implement the blue flux “veto” criterion, we used a weighted sum of six NOAO Deep Wide-Field Survey (NDWFS; Jannuzi & Dey 1999) and LALA survey filters blueward of 6850\AA , where the Lyman break would fall for galaxies whose Lyman- α line falls within the 9180\AA narrowband. The weights were chosen to achieve optimal depth for objects of approximately median color. Most of the weight in this combined “veto image” comes from the NDWFS B_W filter, with additional contributions from NDWFS R band data and the LALA survey’s V band, and three of the redshifted $H\alpha$ narrowband filter observations. This stack reaches a final 2σ limiting AB magnitude of 27.1 at an effective central wavelength near 5000\AA . Formally, some flux may be expected in the R band filter for $z \approx 6.5$ sources, but in practice, intergalactic hydrogen absorption attenuates this flux so severely that it is quite safe to include R band data in the veto stack as we have done.

Photometry for candidate selection was done using SExtractor. All color tests were applied using a 9 pixel diameter aperture, corresponding to $2.32''$, and using SExtractor’s two-image mode to ensure photometry from the same regions in all filters.

In addition to high redshift Lyman- α sources, three types of contaminants may enter the sample. The first is noise spikes in the narrowband image. Assuming Gaussian statistics, we should expect ~ 1 noise peak above our 5σ detection threshold among the $\sim 10^{6.5}$ independent resolution elements in the narrowband image, and more may be found if the noise properties of the image are not perfectly Gaussian. The second is time variable sources (either transient or moving objects). These may mimic emission line objects in our catalog because different filters were observed at widely varying times. For typical LALA survey depths, the expected rate of high redshift supernovae will be ~ 1 per filter per field. The third is low-redshift emission line galaxies of extremely high equivalent width. The expected numbers of such foreground objects are difficult to estimate from either theory or present data—the LALA data themselves are likely to considerably refine the statistics of such contaminating sources.

These criteria yielded a total of three high quality candidate $z \approx 6.5$ Lyman- α galaxies. Formally, six objects passed selection using an old veto filter stack from 2001, but two of these were ruled out completely and a third strongly disfavored by detections in a new NDWFS R band image from 10 April 2002. One of these excluded candidates is almost certainly a supernova at moderate redshift; such an event would not be surprising given the area and depth of our survey. Properties of the four best candidates are summarized in table 1.

4. Keck and Gemini Spectra

Two of the $z=6.5$ candidates (LALA J142441.20+353405.1 and LALA J142544.41+353327.7) were observed using the DEIMOS spectrograph (Faber et al. 2002) on the Keck II telescope of the W. M. Keck Observatory on the night of U.T. 2003 May 01. Observations of LALA J142441.20+353405.1 were also obtained on U.T. 2003 Apr 01. All observations were made using the 600 l/mm ($\lambda_b = 8500\text{\AA}$) grating through slitmasks with slit widths of 1.0arcsec. The total exposure times were broken into individual exposures of 1800s; we performed 2.5 arcsec spatial offsets between exposures to facilitate the removal of fringing at long wavelengths. The nights were clear and the seeing was typically 0.5-0.8arcsec. The data were reduced using the U.C. Berkeley pipeline reduction software (Davis et al. 2004) adapted from programs developed for the SDSS (Burles and Schlegel 2004), and further adapted to our observing mode. The spectra were extracted and analyzed using IRAF (Tody 1993).

The candidates LALA J142441.20+353405.1 and LALA J142442.24+353400.2 were observed on U.T. 2003 May 8 and June 29 using the GMOS spectrograph on Gemini North (Hook et al 2003) in Nod-and-Shuffle mode (Glazebrook & Bland-Hawthorn 2001). The observations were made using the R400+G5305 grating (400 lines/mm, central wavelengths at 756 - 768 nm) through slitmasks with slit widths of 1.0arcsec. On each night, the total exposure time was broken into 5 individual exposures of 900s per nod position. Subsequent exposures were offset by 0.2 arcsec in the spatial direction and 3 nm in wavelength, in order to remove the instrumental features (such as the horizontal stripes in the individual exposures) and to cover the chip gaps. Since the two

Table 1. Photometry

ID	918nm flux (μ Jy)	z' flux (μ Jy)	I flux (μ Jy)	R flux (μ Jy)	Photometric line flux ^a	$W_{\lambda}^{\text{rest}}(2\sigma)$ limit (\AA)	Nature
LALA J142441.20 +353405.1	0.763 ± 0.139	-0.214 ± 0.111	-0.0145 ± 0.045	-0.0372 ± 0.029	4 to 6.6 ^b	> 620	$z = 0.824$
LALA J142442.24 +353400.2	0.767 ± 0.137	-0.081 ± 0.113	-0.064 ± 0.045	-0.061 ± 0.028	2.26 ± 0.40	> 100	$z = 6.535$
LALA J142544.41 +353327.7	0.706 ± 0.138	-0.051 ± 0.106	-0.073 ± 0.044	-0.021 ± 0.029	2.08 ± 0.41		Noise spike
LALA J142610.55 +354557.6	0.797 ± 0.121	-0.137 ± 0.110	0.011 ± 0.046	0.057 ± 0.030	2.35 ± 0.36		Unknown

^aUnits of $10^{-17} \text{ erg cm}^{-2} \text{ s}^{-1}$.

^bThe line for LALA J142441.20+353405.1 falls on the edge of the narrowband filter, where throughput is a rapid function of wavelength. The dominant uncertainty in the photometric line flux is the resulting throughput correction at 9136 \AA , and we quote a range of flux values based on the plausible range of this throughput correction. See text.

Note. — Photometric properties of the candidate $z \approx 6.5$ LALA sources. The 2σ lower bounds on equivalent width are derived from the narrow- and broad-band photometry for LALA J142442.24+353400.2, and from DEIMOS spectra for LALA J142441.20+353405.1, and are corrected to the spectroscopically determined redshift. They are not corrected for IGM absorption, which will affect both the broad and narrow-band photometry of Lyman- α galaxies approximately equally if the unabsorbed line profiles are centered on zero velocity.

objects appear on both the target and sky exposures (i.e., on both shuffle A and shuffle B), the effective exposure time for the two sources are 9000s or 2.5 hours per night, for a grand total of 5 hours' on-source integration.

Additionally, a second GMOS slit mask was observed for a total of 3.5 hours total integration time on UT 2003 July 02 (0.5 hour) and July 03 (3.0 hours), covering the (lower grade) candidate LALA J142610.55+354557.6.

The data were reduced using the Gemini GMOS packages (v1.4) within IRAF through the standard procedures (<http://www.gemini.edu/>). The wavelength calibrations were performed based on the CuAr lamp spectra and were double checked against the night sky lines. The uncertainties in the extracted spectra were obtained empirically by measuring the RMS flux among all spatially distinct pixels at each wavelength in the rectified 2-D spectra.

Additional targets were of course included on all slit masks, including lower redshift emission line galaxies, continuum-selected Lyman break galaxies and intermediate redshift elliptical galaxies, and X-ray sources from the 172 ksec LALA Boötes field Chandra ACIS observation (Wang et al. 2003; Malhotra et al. 2003). Results for these other targets will be presented elsewhere.

5. Spectroscopic Results

Two of our candidates, LALA J142442.24+353400.2 and LALA J142441.20+353405.1, yielded emission lines within the bandpass of the narrowband filter. Of these, one (LALA J142442.24+353400.2) is confirmed as a Lyman- α galaxy, while the other (LALA J142441.20+353405.1) is identified as [O III] λ 5007.

LALA J142442.24+353400.2: LALA J142442.24+353400.2 was confirmed by Gemini-N + GMOS on 2003 May 8 and 2003 June 29. No DEIMOS data were obtained for this object in 2003. There is a single isolated emission line at 9160Å, corresponding to $z = 6.535$ (see figures 1, 2). There is no evidence for continuum emission in either our images or GMOS spectrum. The rest frame equivalent width is $> 100\text{\AA}$ at the 2σ level for $z \approx 6.54$, measured here using our LALA survey narrow- and broad-band photometry. The line width in this source could in principle be consistent with [O II] $\lambda\lambda 3726, 3729$. However, this would imply a rest frame equivalent width $> 245\text{\AA}$ (2σ), which is outside the usual range for this line: two large continuum-selected samples (Cowie et al. 1996, Hogg et al. 1998) and one H α line selected sample (Gallego et al. 1996) found no [O II] $\lambda\lambda 3726, 3729$ sources with $\text{EW} > 140\text{\AA}$ and a very small minority with $100 < \text{EW} < 140\text{\AA}$. Additionally, star forming galaxies usually show blue continuum emission, so that our B_w and R filter nondetections again argue against [O II] $\lambda\lambda 3726, 3729$ models.

The LALA J142442.24+353400.2 emission line has a measured width of 13Å FWHM. This substantially exceeds the instrumental resolution (estimated at 6Å based on the GMOS spectrum

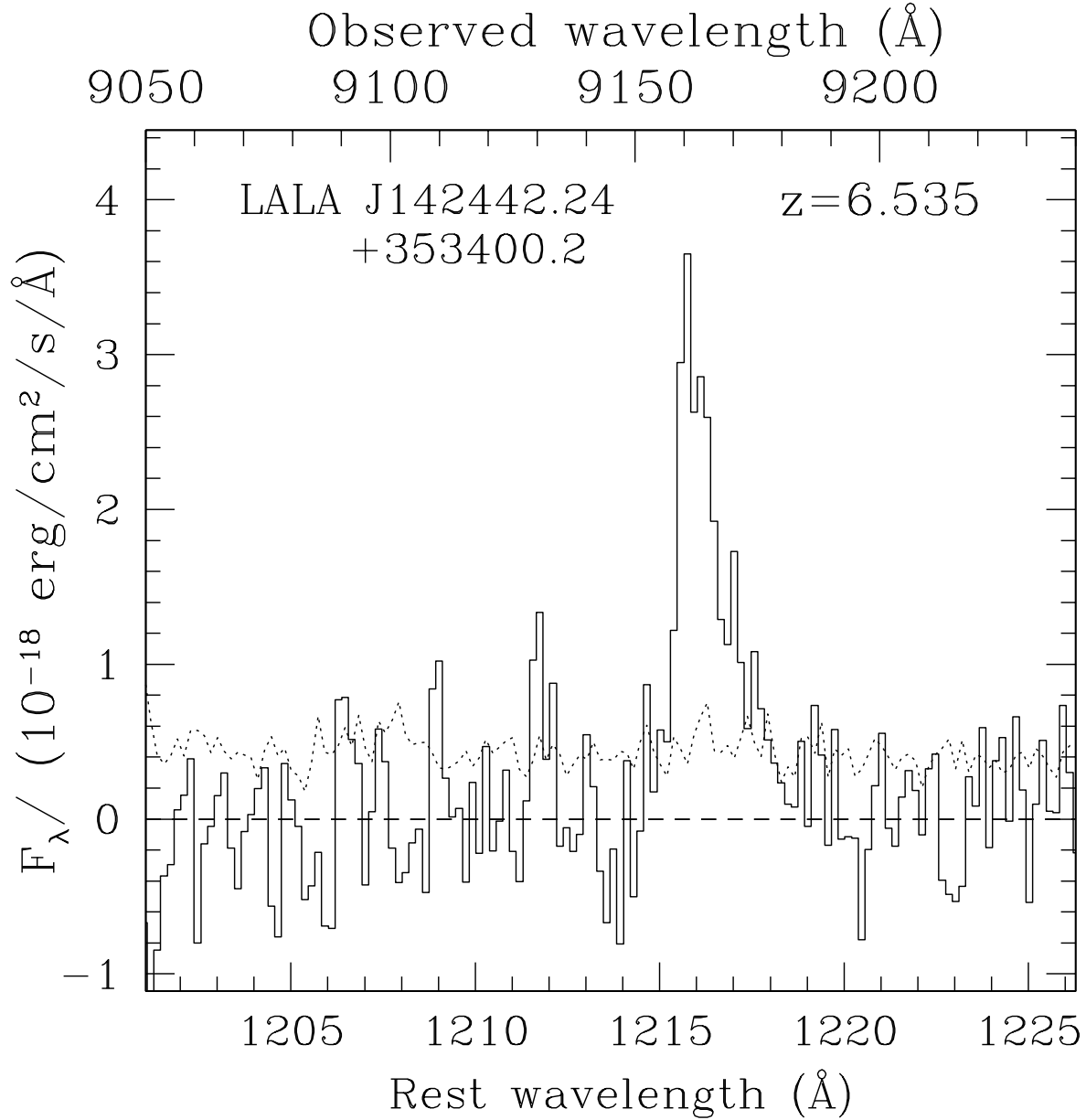


Fig. 1.— Spectrum of LALA J142442.24+353400.2, obtained with the GMOS spectrograph on Gemini North. The solid histogram shows the measured flux; the dotted histogram shows the one-sigma flux uncertainties. The asymmetry of the line is clearly visible. There is no emission at 9072Å, where the [O III] λ 4959 line would be expected if the 9160Å feature were [O III] λ 5007. The conversion from counts to physical units was determined by requiring the integrated line flux to match that determined from our narrowband photometry.

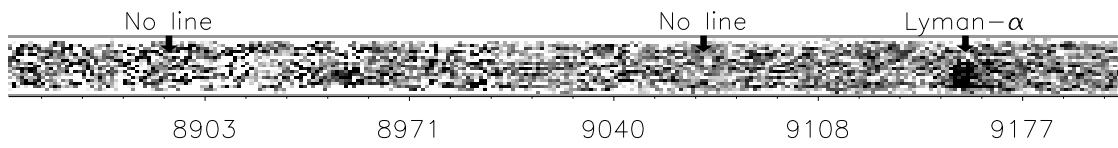


Fig. 2.— 2 dimensional GMOS spectrum of LALA J142442.24+353400.2. Night sky lines are well subtracted here, but their locations are plainly visible as bands of enhanced photon noise. Arrows mark the locations where the H β and [O III] λ 4959 lines would be expected if the primary line at 9160Å were [O III] λ 5007.

of LALA J142441.20+353405.1), and thus allows quantitative asymmetry measurements. The line can be well fit with a truncated gaussian model of the form suggested by Hu et al. (2004): The profile is taken to be a Gaussian of width σ_1 on the red side of a peak wavelength λ_0 and a step function to zero intensity blueward of the peak, but then convolved with a second Gaussian of width σ_2 to reflect instrumental resolution effects. In LALA J142442.24+353400.2, we obtain $\chi^2/\text{(degree of freedom)} = 0.93$ using $\sigma_1 = 8\text{\AA}$, $\sigma_2 = 1.2\text{\AA}$, and $\lambda_0 = 9158\text{\AA}$.

We have further developed the asymmetry statistics a_λ and a_f that were presented in Rhoads et al. (2003). These statistics depend on determination of the wavelengths λ_p where the line flux peaks and $\lambda_{10,b}$, $\lambda_{10,r}$ where the flux drops to 10% of its peak value. To mitigate the effects of noise in the spectrum, all three wavelengths can be measured after a light smoothing. The asymmetry statistics are then defined as $a_\lambda = (\lambda_{10,r} - \lambda_p) / (\lambda_p - \lambda_{10,b})$ and $a_f = \int_{\lambda_p}^{\lambda_{10,r}} f_\lambda d\lambda / \int_{\lambda_{10,b}}^{\lambda_p} f_\lambda d\lambda$. To determine the appropriate smoothing, we simulated observations of a line having the truncated gaussian profile described above and the (wavelength-dependent) noise level achieved in our GMOS data. We find that the asymmetry of the line is most reliably recovered using a Gaussian smoothing near 3 pixels (FWHM). We also experimented with the threshold level for the λ_b and λ_r measurements, but found no clear benefit to raising this threshold. Using 3 pixel smoothing, we find $a_\lambda = 1.78 \pm 0.71$ and $a_f = 1.54 \pm 0.53$, where the error bars are drawn from simulated spectra and defined as a “percentile-based sigma,” i.e., 84% of simulated spectra lie within $\pm\delta\sigma$ of the median simulated a statistic. Thus, the formal asymmetry of this line is just over 1σ .

Given that we see no other significant lines in the spectrum of LALA J142442.24+353400.2, we can rule out [O III] $\lambda 5007$ and H α interpretations quite strongly. The remaining possibility, besides Lyman- α , is [O II] $\lambda\lambda 3726, 3729$. However, the line ratio for [O II] $\lambda\lambda 3726, 3729$ sources under usual astrophysical conditions is $f_{3729}/f_{3726} \approx 1.3$, yielding an asymmetry opposite that of Lyman- α when the doublet is blended. We have tried modelling the data with [O II] $\lambda\lambda 3726, 3729$ doublets. Fixing the line ratio at 1.3 makes it impossible to achieve $\chi^2/\text{d.o.f.} \lesssim 1.9$, clearly worse than the truncated Gaussian model for Lyman- α . If we allow the line ratio to vary arbitrarily, we can achieve $\chi^2/\text{d.o.f.} = 1.0$, but only for $f_{3729}/f_{3726} \approx 0.4$, which would require very unusual physical conditions. If we fix the line ratio at 1.3 we find that simulated spectra yield $a_\lambda(\text{O II}) > 1.78$ in only 6.7% of simulations. The corresponding probability for a_f is slightly higher at 12.9%. Thus, the best interpretation of this line is clearly Lyman- α , from both its asymmetry and its equivalent width.

LALA J142441.20+353405.1: The second of these galaxies, LALA J142441.20+353405.1, was spectroscopically detected in both our Keck + DEIMOS and Gemini-N + GMOS data. A strong emission line is seen at a wavelength 9136\AA . This line is most likely [O III] $\lambda 5007$ at a redshift $z = 0.824$, based on a careful search for other emission lines. Unfortunately, the expected locations of the [O III] $\lambda 4959$ and H β lines both fall atop night sky OH emission features. The interpretation of this object depends critically on these features (with Lyman- α being the best interpretation if no secondary lines exist).

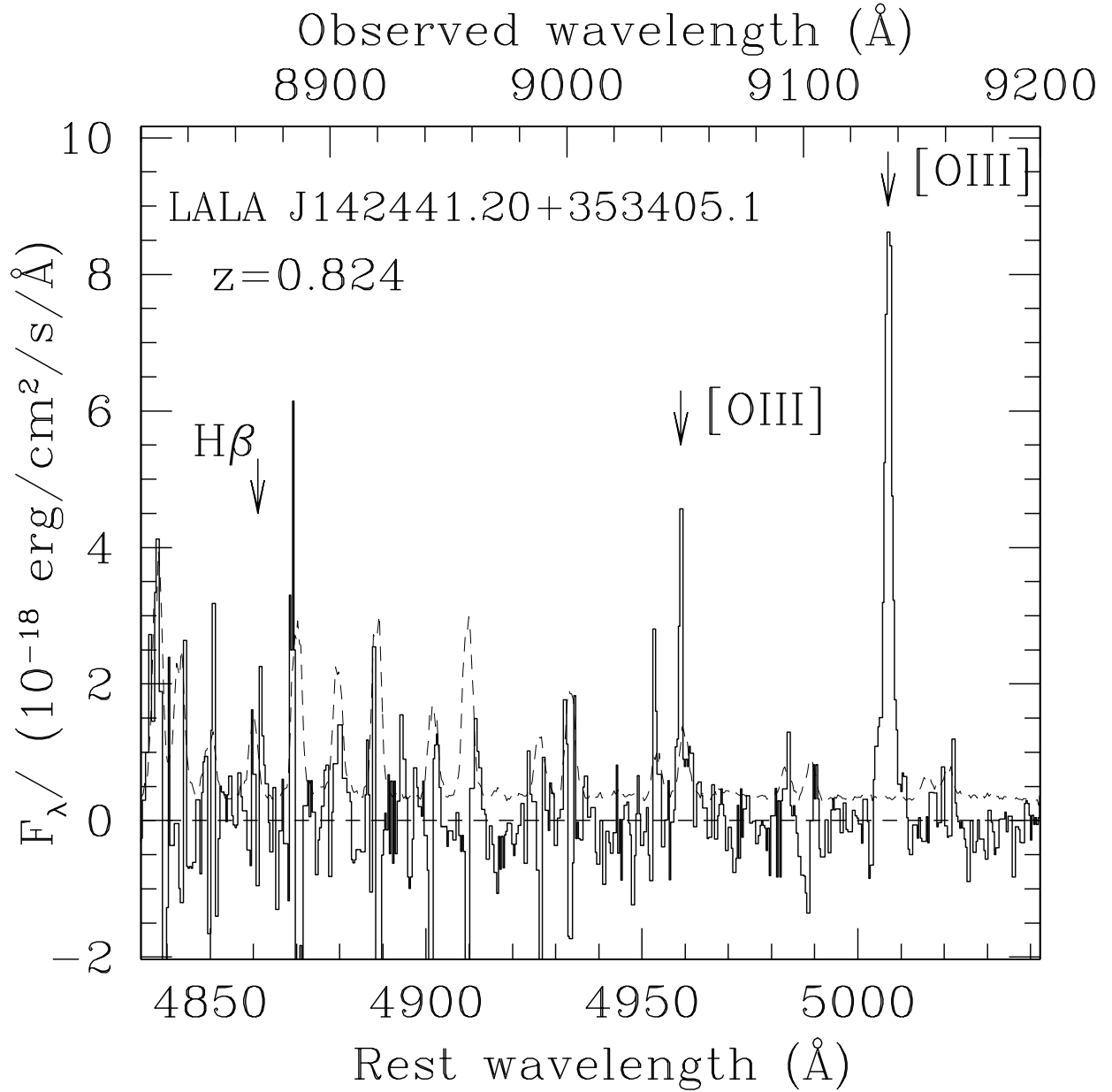


Fig. 3.— Spectrum of LALA J142441.20+353405.1, obtained with the DEIMOS spectrograph on Keck II. The solid histogram shows the measured flux after smoothing with a 3 pixel median filter to suppress residual features from night sky lines. We have marked the wavelengths where the [O III] $\lambda 4959$ and $H\beta$ lines would fall if the primary line at 9136Å is [O III] $\lambda 5007$.

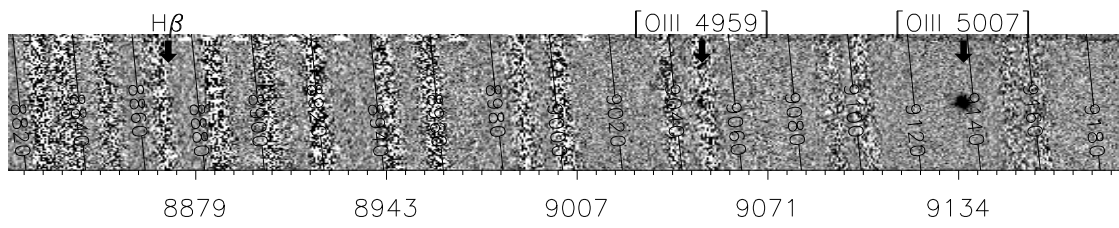


Fig. 4.— 2 dimensional DEIMOS spectrum of LALA J142441.20+353405.1. Labeled contours show the wavelength scale. Night sky lines are well subtracted here, but their locations are plainly visible as bands of enhanced photon noise. The presumed [O III] $\lambda 4959$ line is at 9048Å, and is partly visible to the blue of the 9049Å night sky line. The expected location of H β is at 8870Å.

We therefore fitted Gaussian line profiles at the expected locations of both [O III] $\lambda 4959$ and $H\beta$, using fitting weights derived from the observed profile of the 9136Å line and from the observed noise as a function of wavelength in sky-subtracted spectra. This approach optimally exploits any part of the satellite line profile that is not obscured by night sky line residuals. We obtained a four sigma detection of the [O III] $\lambda 4959$ line and a line flux ratio of 0.33 ± 0.08 ($f(4959)/f(5007)$) from our 2-D DEIMOS data. A similar exercise using the 1-D GMOS data gave another 4σ detection at the expected [O III] $\lambda 4959$ wavelength and a line ratio of 0.35 ± 0.09 . The consistency of these results with one another and with the theoretically expected line ratio of 0.33 leads us to believe this interpretation of the data. Further fitting yields also a marginal $H\beta$ detection in the DEIMOS data (3σ , line ratio 0.111 ± 0.04) but nothing significant in the GMOS data. Measurement of the [O II] $\lambda\lambda 3726, 3729$ lines with this method is more difficult, since the expected position of [O II] $\lambda\lambda 3726, 3729$ depends on the spectral trace (which we cannot measure because the continuum in LALA J142441.20+353405.1 is undetected). In practice, we see a hint of the [O II] $\lambda\lambda 3726, 3729$ doublet in both data sets, but it is more significant in the GMOS data (2.4σ and 6.4σ for 3726Å and 3729Å) than in the DEIMOS data (3.7σ and 1.0σ). Further circumstantial support for the $z = 0.824$ interpretation comes from spectroscopic observations of a red galaxy sample in this field, which show a strong spike in the redshift distribution at $z \approx 0.824$ (Dey et al. 2004).

Other foreground emission line interpretations are ruled out: An $H\alpha$ line at 9136Å should imply [O III] $\lambda\lambda 4959, 5007$ and $H\beta$ near 6900Å, which is not seen, and [O II] $\lambda\lambda 3726, 3729$ at 9136Å would be easily resolved as a close doublet in our DEIMOS data.

The flux of the 9136Å line is large but subject to systematic uncertainties. Flux standards from our DEIMOS run imply a line flux of $3 \lesssim f_{17} \lesssim 5.7$, where $f_{17} \equiv f/(10^{-17} \text{ erg cm}^{-2} \text{ s}^{-1})$ is the scaled line flux. Our LALA survey narrowband imaging would naïvely imply a flux $f_{17} = 2.2$, but the measured wavelength places the emission line on the wing of the narrowband filter, where the throughput is low. Correcting by a factor $T_{max}/T(9136\text{\AA})$ implies a line flux $4 \lesssim f_{17} \lesssim 6.6$, where the lower value is based on the original filter specifications given to the vendor and the higher value is based on filter tracings made in May 2003 at NOAO by Heidi Schweiker and George Jacoby. We adopt $f_{17} = 4$ as a reasonable best guess. We do not see statistically significant evidence for line asymmetry, which is hardly surprising given the line width. We also see no evidence for continuum emission. The best equivalent width estimate for this source comes from our DEIMOS data, which yield a 2σ lower bound of $EW > 620\text{\AA}$ in the rest frame for $z = 0.824$.

LALA J142441.20+353405.1 and LALA J142442.24+353400.2 lie $13''$ apart, corresponding to a projected separation of $\approx 80\text{kpc}$ (non-comoving). This proximity appears to be a coincidence given the differing line identifications. If the lines were the same transition, the velocity separation of the two would be $\approx 800\text{km s}^{-1}$.

Other candidates: Of the remaining two candidates, LALA J142544.41+353327.7 was detected only in the 918nm filter and is probably a noise spike in that filter, based on its nondetection in

Keck DEIMOS data. Assuming Gaussian statistics, we should expect ~ 1 noise peak above our 5σ detection threshold among the $\sim 10^{6.5}$ independent resolution elements in the narrowband image, and more may be found if the noise properties of the image are not perfectly Gaussian. The second spectroscopic nondetection, LALA J142610.55+354557.6, may have been a time-variable continuum source rather than a true emission line object. It was targeted in a GMOS mask observed on 2003 July 02 and 03, with a total integration time exceeding that required to detect LALA J142441.20+353405.1 and LALA J142442.24+353400.2, which have similar narrowband fluxes. It appears as a narrowband excess target when compared to images from 2001 and before, but has a marginal R band detection in NDWFS images from UT 2002 April. This R band detection is offset from the 918nm source by about $0.8''$, and may or may not be the same source, since the faintness of the object renders precise narrowband astrometry difficult. Regardless of its precise nature, it appears not to be a redshift 6.5 Lyman- α galaxy.

6. Discussion

6.1. Physical Parameters of the Sources

Adopting a cosmology with $\Omega_m = 0.27$, $\Omega_\Lambda = 0.73$, and $H_0 = 71 \text{ km s}^{-1} \text{ Mpc}^{-1}$ (cf. Spergel et al. 2003) gives a luminosity distance of $2.00 \times 10^{29} \text{ cm}$ (65Gpc) for $z \approx 6.53$. We then obtain a line luminosity of $1.1 \times 10^{43} \text{ erg s}^{-1}$ for LALA J142442.24+353400.2. Comparing with a Lyman- α luminosity function at $z \approx 6.5$ that we derive in a companion paper (Malhotra et al. 2004, hereafter M04), we find that LALA J142442.24+353400.2 has about six times the characteristic Lyman- α luminosity $L_{Ly\alpha,*}$ of emission line selected galaxies at this redshift.

We can convert this to an estimated star formation rate using a conversion factor of $1M_\odot/\text{yr} = 10^{42} \text{ erg s}^{-1}$, which yields $11 M_\odot/\text{yr}$. This conversion follows from a widely used set of assumptions: a Kennicutt (1983) initial mass function (IMF) and corresponding conversion between H α luminosity and star formation rate, plus the Lyman- α to H α ratio for dust-free case B recombination. These are probably not valid in detail for high redshift Lyman- α galaxies, but as we do not yet have a well justified model, it is convenient to at least use a standard one. Combined with our survey volume of $2.1 \times 10^5 \text{ Mpc}^3$ (comoving), we obtain a lower bound on the star formation rate density (SFRD) of $5.2 \times 10^{-5} M_\odot \text{ yr}^{-1} \text{ Mpc}^{-3}$ from LALA J142442.24+353400.2 alone. Of course, given that LALA J142442.24+353400.2 is much brighter than L_* , its contribution to the star formation rate density is only a small fraction of the total.

For LALA J142441.20+353405.1, we have flux measurements or limits on the [O III] $\lambda 5007$, [O II] $\lambda 3727$, and H β transitions. These allow us to place general constraints on the metallicity of this galaxy using $R_{23} \equiv \log([f(5007) + f(4959) + f(3727)]/f(H\beta))$. We then have $R_{23} \geq \log([f(5007) + f(4959)]/f(H\beta)) = 1.1 \pm 0.12$. The additional contribution to the oxygen flux from [O II] $\lambda 3727$ is either negligible (using the DEIMOS measurement, $\log([\text{O II}]/[\text{O III}]) = -1.3$) or small (using the GMOS measurement, -0.4). From Kewley & Dopita (2002), the theoretical

maximum for R_{23} is 0.97, achieved only for a modestly sub-solar metallicity near $\log(O/H) + 12 \approx 8.38$ and a high ionization parameter $q > 3 \times 10^8$. Our observation is consistent with this theoretical maximum, but not with R_{23} substantially below this maximum, and we thus conclude that LALA J142441.20+353405.1 has $\log(O/H) + 12 \approx 8.4$ (which is about 0.5 dex below the solar O/H ratio).

6.2. Implications for Reionization

Because Lyman- α photons are resonantly scattered by neutral hydrogen, Lyman- α emitting galaxies may suffer considerable attenuation of their line flux when embedded in an intergalactic medium (IGM) with a substantial neutral fraction. Thus, a decrease in Lyman- α galaxy counts may be expected at redshifts substantially before the end of reionization (Rhoads & Malhotra 2001, Hu et al. 2002, Rhoads et al. 2003). Typical high redshift Lyman- α galaxies have small continuum fluxes, and upper limits can be placed on their expected Stromgren sphere radius r_s by combining their observed fluxes and equivalent widths with stellar population models (Rhoads & Malhotra 2001). A radius of $r_s \sim 0.5\text{Mpc}$ is typically inferred. For comparison, $r_s > 1.2\text{Mpc}$ is required to avoid a scattering optical depth $\tau > 1$ at emitted line center due to the neutral IGM outside the Stromgren sphere.

Haiman (2002) has argued that the first reported $z \approx 6.5$ galaxy (Hu et al. 2002) could still be embedded in a neutral IGM, because (a) emission from the red wing of the emitted line will be less strongly scattered than line center, reducing the effective attenuation of the line, and (b) the observed Lyman- α equivalent width in this object is substantially below the theoretical maximum from stellar population models, so that the observed line could in fact be substantially attenuated. Santos (2003) considers additional physical effects, including gas motions and overdensity associated with the formation of Lyman- α galaxies, which generally increase the Lyman- α attenuation over that in Haiman’s model. However, Santos also suggests that the velocity differences observed between Lyman- α lines and other emission lines in Lyman break galaxies could be intrinsic to the source, so that the entire Lyman- α line is emitted with an effective redshift of a few hundred km s^{-1} . In this case, the effective Lyman- α attenuation for $z \sim 6.5$ is a factor of ~ 3 , and is not very sensitive to model parameters besides the ionization state of the IGM.

LALA J142442.24+353400.2 places stronger constraints on reionization models than previously discovered $z \approx 6.5$ galaxies because of its large equivalent width ($> 100\text{\AA}$ rest frame, 2σ). In a neutral universe, this would require an intrinsic equivalent width $\gtrsim 300\text{\AA}$ even if the Lyman- α line is redshifted as suggested by Santos, and $\gtrsim 1000\text{\AA}$ in the absence of such a redshift. The former is consistent with the observed Lyman- α equivalent width distribution at $z \approx 4.5$ (Malhotra & Rhoads 2002), though difficult to explain with conventional stellar population models. The latter is extreme even for the $z \approx 4.5$ sample. Thus, the properties of this object are most easily understood if the universe is mostly ionized at $z \approx 6.5$. More robust constraints on reionization from *individual* Lyman- α galaxies will be difficult, because the expected suppression of the Lyman- α line depends

strongly on the velocity offset between emitted Lyman- α and the galaxy’s systemic velocity, and measuring the latter would in general require spectroscopy in the thermally dominated mid-infrared (Santos 2003).

Stronger constraints on reionization from Lyman- α galaxies will be possible using statistical samples. Suppression of Lyman- α by the IGM will have a strong effect on the Lyman- α luminosity function: Even a factor of ~ 3 reduction in Lyman- α flux will reduce the observed Lyman- α number counts dramatically. The accessible portion of the Lyman- α luminosity function is very steep (see Malhotra et al. 2004), and a factor of 3 in luminosity threshold corresponds to a factor of $\gtrsim 10$ in expected Lyman- α source counts at fixed sensitivity. Moreover, the effect on the equivalent width distribution will be identical to that on the luminosity function, which would not be generically expected for other factors that could modify the Lyman- α luminosity function (such as evolution).

7. Conclusions

We have performed a narrowband search for Lyman- α emitting galaxies at $z \approx 6.5$ in the Boötes field of the Large Area Lyman Alpha survey, and have obtained spectra for all of our viable candidates. One source, LALA J142442.24+353400.2, is confirmed as Lyman- α at $z = 6.535$, based on an isolated, asymmetric emission line. The Lyman- α luminosity of this source is large, $\sim 6L_{Ly\alpha,*}$, implying that it is an unusual and rare object. It is therefore likely to correspond to a high peak in the density distribution at redshift $z = 6.535$. The equivalent width is also larger than most other $z \approx 6.5$ galaxies, with a lower bound of $> 100\text{\AA}$ (rest frame). This is difficult to reconcile with a neutral intergalactic medium unless the Lyman- α line is intrinsically very strong *and* is emitted from its host galaxy with an intrinsic Doppler shift of several hundred km s^{-1} .

We thank Paul Groot and collaborators for their help in obtaining some of our June 2001 imaging data; Richard Green, Jim De Veny, and Bruce Bohannon for their support of the LALA survey; and Heidi Schweiker and George Jacoby for help with filter curve measurements. This work made use of images provided by the NOAO Deep Wide-Field Survey (Jannuzi and Dey 1999), which is supported by the National Optical Astronomy Observatory (NOAO). We thank Melissa Miller, Alyson Ford, Michael J. I. Brown, and the rest of the NDFWS team for their work on the NDFWS data. NOAO is operated by AURA, Inc., under a cooperative agreement with the National Science Foundation. STScI is operated by the Association of Universities for Research in Astronomy, Inc., under NASA contract NAS5-26555. The analysis pipeline used to reduce the DEIMOS data was developed at UC Berkeley with support from NSF grant AST-0071048. The work of S. D. was supported by IGPP-LLNL University Collaborative Research Program grant 02-AP-015 and was performed under the auspices of the Department of Energy, National Nuclear Security Administration, by the University of California, Lawrence Livermore National Laboratory, under contract W-7405-Eng-48. H. S. thanks the National Science Foundation for support under NSF grant AST-0097163. The work of D. S. was carried out at Jet Propulsion

Laboratory, California Institute of Technology, under a contract with NASA. The authors wish to recognize and acknowledge the very significant cultural role and reverence that the summit of Mauna Kea has always had within the indigenous Hawaiian community. We are most fortunate to have the opportunity to conduct observations from this mountain.

REFERENCES

Becker, R. H. et al. 2001, AJ 122, 2850

Burles, S., & Schlegel, D., 2004, in preparation

Cash, W. 1979, ApJ, 228, 939

Connolly, A. J., Szalay, A. S., Dickinson, M., SubbaRao, M. U., & Brunner, R. J. 1997, ApJ 486, L11

Cowie, L. L., Songaila, A., Hu, E. M., & Cohen, J. G. 1996, AJ 112, 839

Cuby, J.-G., LeFevre, O., McCracken, H., Cuillandre, J.-C., Magnier, E., & Meneux, B. 2003, A&A 405, L19

Davis, M., et al. 2004, in preparation

Dawson, S., et al. 2004, in preparation

Dey, A., et al. 2004, in preparation.

Faber, S., et al. 2002, Proc. SPIE, 4841, 1657

Fan, X., Narayanan, V. K., Strauss, M. A., White, R. L., Becker, R. H., Pentericci, L., & Rix, H.-W. 2002, AJ 123, 1247

Fischer, P., & Kochanski, G. P. 1994, AJ 107, 802

Gallego, J., Zamorano, J., Rego, M., Alonso, O., & Vitores, A. G. 1996, A&AS 120, 323

Glazebrook, K., & Bland-Hawthorn, J. 2001, PASP 113, 197

Haiman, Z. 2002, ApJ 576, L1

Hogg, D.W., Cohen, J.G., Blandford, R. & Pahre, M.A. 1998, ApJ, 504, 622

Holder, G. Haiman, Z., & Mohr, J. J. 2001, ApJ 560, L111

Hook, I. et al. 2003, Proc. SPIE, 4841, 1645

Hu, E. M., Cowie, L. L., McMahon, R. G., Capak, P., Iwamuro, F., Kneib, J.-P., Maihara, T., Motohara, K. 2002, ApJ 568, L75

Hu, E. M., Cowie, L. L., Capak, P., McMahon, R. G., Hayashino, T., & Komiyama, Y. 2004, ApJ, in press; astro-ph/0311528

Hui, L., & Haiman, Z. 2003, ApJ 596, 9

Jannuzi, B. T. & Dey, A., 1999, in “Photometric Redshifts and the Detection of High Redshift Galaxies,” ASP Conference Series Vol. 191, Edited by R. Weymann, L. Storrie-Lombardi, M. Sawicki and R. Brunner. ISBN: 158381-017-X, p. 111

Kennicutt, R. C., Jr. 1983, ApJ 272, 54

Kewley, L. J., & Dopita, M. A. 2002, ApJS 142, 35

Kneib, J.-P., Ellis, R. S., Santos, M. R., & Richard, J. 2004, astro-ph/0402319

Kodaira, K., et al. 2003, PASJ 55, L17

Madau, P., Ferguson, H. C., Dickinson, M. E., Giavalisco, M., Steidel, C. C., Fruchter, A. 1996, MNRAS 283, 1388

Madau, P., & Shull, J. M. 1996, ApJ 457, 551

Malhotra, S., & Rhoads, J. E. 2002, ApJ 565, L71

Malhotra, S., Wang, J. X., Rhoads, J. E., Heckman, T. M., & Norman, C. A. 2003, ApJ 585, L25

Monet, D. B. A., et al 1998, “The USNO-A2.0 Catalogue,” VizieR Online Data Catalogue

Peebles, P. J. E., 1993, *Principles of Physical Cosmology*, Princeton: Princeton University Press

Rhoads, J. E., Malhotra, S., Dey, A., Stern, D., Spinrad, H., & Jannuzi, B. T. 2000, ApJ 545, L85

Rhoads, J. E. 2000, PASP 112, 703

Rhoads, J. E., & Malhotra, S. 2001, ApJ 563, L5

Rhoads, J. E., Dey, A., Malhotra, S., Stern, D., Spinrad, H., Jannuzi, B. T., Dawson, S., Brown, M. J. I., & Landes, E. 2003, AJ 125, 1006

Santos, M. R. 2003, astro-ph/0308196

Spergel, D. N., et al. 2003, ApJS, 148, 175

Stanway, E., Bunker, A., & McMahon, R. G. 2003, MNRAS 342, 439

Theuns, T., Schaye, J., Zaroubi, S., Kim, T.-S., Tzanavaris, P., & Carswell, R. 2002, ApJ 576, L103

Tody, D., 1993, in ASP Conf. Ser. 52 ”Astronomical Data Analysis Software and Systems II, ed. R. Hanisch, R. Brissenden, & J. Barnes (San Francisco, ASP), 173

Valdes, F., & Tody, G. 1998, Proceedings of SPIE Vol. 3355

Valdes, F. 1998, ADASS VII, ASP Conf. Series 145, ed. R. Albrecht

Wang, J. X., Malhotra, S., Rhoads, J. E., Brown, M. J. I., Dey, A., Heckman, T. M., Jannuzi, B. T., Norman, C. A., Tiede, G. P., & Tozzi, P. 2003, AJ, in press, astro-ph/0309705